Semi-empirical calculation of K to L_i sub-shell, K to L, and M shell vacancy transfer probability for elements in the atomic range $16 \leq Z \leq 92$

B. Berkani[1,2], A. Kahoul[1,2*], J.M. Sampaio[3,4], S. Daoudi[1,2], J.P. Marques[3,4], F. Parente[5], A. Hamidani[1,2], S. Croft[6], A.Favalli[7,8], Y. Kasri[9,10], A. Zidi[1,2], K. Amari[1,2]

[1]*Department of Matter Sciences, Faculty of Sciences and Technology, Mohamed El Bachir El Ibrahimi University, Bordj-Bou-Arreridj 34030, Algeria.*
[2]*Laboratory of Materials Physics, Radiation and Nanostructures (LPMRN), Faculty of Sciences and Technology, Mohamed El Bachir El Ibrahimi University, Bordj-Bou-Arreridj 34030, Algeria.*
[3]*LIP – Laboratório de Instrumentação e Física Experimental de Partículas, Av. Prof. Gama Pinto 2, 1649-003 Lisboa, Portugal.*
[4]*Faculdade de Ciências da Universidade de Lisboa, Campo Grande, C8, 1749-016 Lisboa, Portugal.*
[5]*Laboratory of Instrumentation, Biomedical Engineering and Radiation Physics (LIBPhys-UNL), Department of Physics, NOVA School of Science and Technology, NOVA University Lisbon, 2829-516 Caparica, Portugal.*
[6]*School of Engineering, Faculty of Science of Technology, Nuclear Science & Engineering Research Group, Lancaster University, Bailrigg, Lancaster, LA1 4YW, United Kingdom.*
[7]*European Commission, Joint Research Centre, Ispra, I-21027, Italy.*
[8]*Los Alamos National Laboratory, P.O. Box 1663, Los Alamos, NM 87545, USA.*
[9]*Department of Physics, Faculty of Sciences, University of Mohamed Boudiaf, 28000 M'sila, Algeria.*
[10] *Theoretical Physics Laboratory, Faculty of Exact Sciences, Bejaia University, 06000 Bejaia, Algeria.*
[*]Corresponding author. Tel. /Fax (+213) 035862230.
E-mail address: a.kahoul@univ-bba.dz

Abstract:

This study introduces novel semi-empirical calculations to obtain vacancy transfer probabilities from the K shell for elements in the atomic range $16 \leq Z \leq 92$. These calculations are derived from experimental data extracted from the scientific literature and previously tabulated by the research team. The results are compared with theoretical, semi-empirical, and experimental values reported in the literature, demonstrating a good agreement between the obtained findings and those of previous works.

Keywords: Semi-empirical calculation, vacancy transfer probabilities, weighted average values.

1. Introduction

Utilizing both theoretical and experimental methods, along with fitting empirical and semi-empirical formulae to experimental data, is paramount in determining vacancy transfer probabilities, particularly with K-shell vacancies across various elements. This significance arises from their numerous applications in physics, chemistry, medical research, and nuclear science and technology. Their utility extends to fields such as X-ray spectroscopy, which is crucial for nuclear safeguards, safety, and security applications, as well as plasma physics, astrophysics, materials science, radiation dosimetry, plasma characterization, radiation protection, and industrial radiation processing. Vacancy transfer is intricately tied to the interaction of photons with matter, which can occur through various mechanisms largely dependent on the energy of the incident photons. Central to this interaction is photoionization, wherein a bound electron is ejected, leaving behind a vacancy that is subsequently occupied by an electron from a higher-energy shell. The nature of this transition, whether radiative or nonradiative, is governed by quantum mechanical principles known as selection rules (Turşucu et al. 2012). Numerous researchers have undertaken calculations to assess vacancy transfer probabilities from the K-shell to the *X*-shell/subshell (*X* = L, M). Experimental measurements of vacancy transfer probabilities from the K shell using various methods have been reported (Akman 2016a, 2016b; Alım *et al*. 2017a, 2017b; Anand *et al*. 2018, 2015, 2014, 2013, 2012; Apaydın and Tıraşoğlu 2012; Aylikci *et al.* 2015; Baydaş 2005; Bennal *et al.* 2010; Çalişkan *et al.* 2002; Cengiz *et al.* 2011, 2010, 2008; Demir and Şahin 2007; Durak *et al.* 2012; Durak and Özdemir 2000, 1998; Durdu *et al.* 2022; Ertuğral *et al*. 2010, 2006, 2005, 2003; Ertuğrul 2003, 2002a, 2002b, 2002c, 2002d; Ertuğrul *et al*. 1997a, 1997b; George *et al*. 2014; Gudennavar and Bubbly 2023; Han *et al*. 2007; Han and Demir 2010; Kaya *et al*. 2014; Mirji *et al*. 2015a, 2015b; Onder *et al.* 2013; Öz, 2006; S. Puri *et al*. 1993; Rao *et al*. 1972; Reyes-Herrera and Miranda 2009, 2008; Santra *et al.* 2005; Schönfeld and JanBen 1996; Şimşek *et al*. 2003; Söğüt 2009,

2006; Söğüt *et al*. 2009; Sreevidya *et al*. 2014; Turhan *et al*. 2020, 2017; Turhan and Akman 2023; Turşucu *et al*. 2013, 2012; Turşucu and Demir 2013; Uğurlu *et al*. 2020; Uğurlu and Demir 2020). These methods vary depending on experimental conditions such as the ionization process, target material, and detectors employed. Rao *et al*. (1972) specifically focused on determining the average number of primary L_i subshell vacancies resulting from transitions to the K-shell across elements with atomic numbers ranging from 20 to 96, while Bambynek *et al.* (1972) provided a comprehensive review. Puri *et al*. (1993) conducted calculations for the total K-to-L_1, L_2, and L_3 subshell probabilities (η_{KL_i}) for elements with atomic numbers ranging from 18 to 96, employing theoretical radiative transition rates from Scofield (1974), and radiationless transition rates tabulated by Chen *et al.* (1979). Schönfeld and JanBen (1996) compiled semi-empirical data in a table for K-to-L-shell (η_{KL}^{T}) total vacancy transfer probabilities, covering elements with atomic numbers from 10 to 100. Aylikci *et al.* (2015) calculated empirical and semi-empirical η_{KL}^{T}values for the elements with atomic numbers $21 \leq Z \leq 30$. Berkani *et al*. (2024) presented total empirical vacancy transfer probabilities η_{KL}^{T} for elements with $16 \leq Z \leq 92$, and radiative transfer probabilities η_{KL2}^{R} and η_{KL3}^{R} for $23 \leq Z \leq 92$, and η_{KM}^{R} for $24 \leq Z \leq 92$. These results were based on an existing compilation of experimental data fitted to an analytical function of the atomic number *Z*.

In this paper we present novel semi-empirical calculations for atomic parameters η_{KL}^{T}, η_{KL2}^{R}, η_{KL3}^{R}, and η_{KM}^{R}, pertinent to vacancy transfer probabilities. These calculations are based on meticulously tabulated experimental data collected from the scientific literature by the research group (Berkani *et al*. 2024). A total of 413 values for η_{KL}^{T} were compiled from 49 papers, covering studies conducted between April 1993 and June 2023 by several researchers (Akman 2016b, 2016a; Alım *et al.* 2017b, 2017a; Anand et al. 2018, 2015, 2014, 2013, 2012; Apaydın and Tıraşoğlu 2012; Aylikci *et al*. 2015; Baydaş 2005; Bennal *et al*. 2010; Cengiz *et al*. 2011, 2010, 2008; Durdu *et al*. 2022; Ertuğral *et al*. 2010, 2006, 2005, 2003; Ertuğrul 2003, 2002c,

2002b, 2002a; Ertuğrul *et al*. 1997b; George *et al*. 2014; Gudennavar and Bubbly, 2023; Han *et al*. 2007; Han and Demir 2010; Kaya *et al*. 2014; Mirji *et al*. 2015a, 2015b; Onder *et al*. 2013; Öz 2006; S. Puri et al. 1993; Santra *et al*. 2005; Şimşek *et al*. 2003; Söğüt 2009, 2006; Söğüt *et al*. 2009; Sreevidya *et al*. 2014; Turhan *et al*. 2020; Turhan and Akman 2023; Turşucu *et al*. 2013, 2012; Turşucu and Demir 2013; Uğurlu *et al*. 2020; Uğurlu and Demir 2020). For $\eta_{\mathrm{KL2}}^{\mathrm{R}}$ and $\eta_{\mathrm{KL3}}^{\mathrm{R}}$, a total of 138 values for each parameter were compiled from 20 papers published between February 1997 and December 2017, from different works (Akman 2016b; Anand *et al*. 2014; Bennal and Badiger 2006; Çalişkan *et al*. 2002; Demir and Şahin 2007; Durak *et al*. 2012; Durak and Özdemir 2000, 1998; Ertuğrul 2003, 2002a, 2002b, 2002c, 2002d; Ertuğrul *et al*. 1997a; Reyes-Herrera and Miranda 2009, 2008; Söğüt 2009, 2006; Sreevidya *et al*. 2014; Turhan *et al*. 2017). Additionally, for $\eta_{\mathrm{KM}}^{\mathrm{R}}$, a total of 103 values were gathered from 10 papers published between February 1997 and July 2016, from works of (Akman 2016b; Anand *et al*. 2014; Çalişkan *et al*. 2002; Demir and Şahin 2007; Durak and Özdemir 2000, 1998; Ertuğrul 2002d; Ertuğrul *et al*. 1997a; Söğüt 2006; Sreevidya *et al*. 2014). These semi-empirical calculations cover a broad atomic range, with $\eta_{\mathrm{KL}}^{\mathrm{T}}$ calculated for elements with $16 \leq Z \leq 92$, $\eta_{\mathrm{KL2}}^{\mathrm{R}}$ and $\eta_{\mathrm{KL3}}^{\mathrm{R}}$ for elements with $23 \leq Z \leq 92$, and $\eta_{\mathrm{KM}}^{\mathrm{R}}$ for elements within the range $24 \leq Z \leq 92$. The calculations are carried out using an interpolation procedure, which involves fitting an analytical function, using the weighted average values calculated by Berkani *et al*. (2024) as a function of the atomic number *Z,* and then fitting the experimental to weighted average ratios. The semi-empirical values obtained for a wide range of elements are presented in tabular form, facilitating easy reference and comparison. Additionally, a comprehensive comparison is made with other theoretical, experimental, and semi-empirical values reported in the literature. Notably, a strong correlation is observed between the obtained semi-empirical results and those reported in previous studies, validating the approach efficacy and the accuracy of the semi-empirical calculations.

2. Semi-empirical calculation

Numerous efforts have been undertaken to compute vacancy transfer probabilities, whether through theoretical models or empirical and semi-empirical approaches involving the fitting of experimental data with various functional forms. The K-to-*X*-shell/subshell (*X* = L, M, etc.) vacancy transfer probabilities representing the average number of vacancies generated in the *X*-shell/subshell per vacancy originating in the K-shell, and are defined following (Berkani *et al*. 2025; Sampaio *et al*. 2016) as

$$\eta_{\mathrm{K}X_i} = \frac{\Gamma^{\mathrm{R}}_{\mathrm{K}X_i} + 2\Gamma^{\mathrm{A}}_{\mathrm{K}X_i;X_i} + \sum_{j\left(Y_j \neq X_i\right)} \Gamma^{\mathrm{A}}_{\mathrm{K}X_i;Y_j}}{\Gamma^{\mathrm{R}}_{\mathrm{K}} + \Gamma^{\mathrm{A}}_{\mathrm{K}}}, \tag{1}$$

where $\Gamma^{\mathrm{R}}_{\mathrm{K}X_i}$ is the partial radiative transition rate of a vacancy in the K shell to a vacancy in a X_i subshell, and $\Gamma^{\mathrm{A}}_{\mathrm{K}X_i;Y_j}$ is the partial radiationless transition rate of a K-shell vacancy to a X_i subshell and another vacancy in a X_j subshell ($j \neq i$ if $X = Y$). The statistical weight 2 in the term $\Gamma^{\mathrm{A}}_{\mathrm{K}X_i;X_i}$ takes into account the possibility that radiationless transitions can create two vacancies in the same subshell X_i. Additionally, for *X* = L, M, etc.,

$$\eta^{\mathrm{T}}_{\mathrm{K}X} = \sum\nolimits_i \eta_{\mathrm{K}X_i} \tag{2}$$

Additionally, to empirically fit the experimental vacancy transfer probability data, an empirical formula of the form (Berkani *et al*. 2024)

$$\eta_{\mathrm{emp}} = \sum_{i=0}^{n} A_i \, Z^i \tag{3}$$

is employed, where the coefficients A_0, $A_1 \ldots A_{\mathrm{n}}$, are determined from the experimental data and relate the vacancy transfer probability to the atomic number *Z*.

In this study, a method was employed to deduce the semi-empirical vacancy transfer probabilities as follows: initially, the quantity $\eta_{\mathrm{W}} = \frac{1}{\sum_{i=1}^{N} \frac{1}{\left(\Delta(\eta)_{\mathrm{exp}-i}\right)^2}} \cdot \sum_{i=1}^{N} \frac{\eta_{\mathrm{exp}-i}}{\left(\Delta(\eta)_{\mathrm{exp}-i}\right)^2}$, given in

the texts of Amari *et al*. 2024a, Daoudi *et al*. 2020, Hamidani *et al*. 2023, and *Zidi et al*. 2024, was plotted against *Z*, as shown in Fig. 1a (for $\eta_{\mathrm{KL}}^{\mathrm{T}}$), Fig. 2a (for $\eta_{\mathrm{KL2}}^{\mathrm{R}}$), Fig. 3a (for $\eta_{\mathrm{KL3}}^{\mathrm{R}}$), and Fig. 4a (for $\eta_{\mathrm{KM}}^{\mathrm{R}}$). This quantity was calculated and reported by Berkani *et al*. (2024). Here η_{W} represents the weighted average value, $\eta_{\mathrm{exp}-i}$ denotes the i^{th} experimental value, $\Delta(\eta)_{\mathrm{exp}-i}$ signifies the assigned uncertainty for the i^{th} experimental value, and *N* indicates the number of experimental data points for the element.

Subsequently, these values were fitted using a fourth-order polynomial:

$$\eta_{\mathrm{W}} = A_0 + \sum_{i=1}^{4} A_i Z^i = f(Z) \tag{4}$$

Following this, the ratio $S = \frac{\eta_{\mathrm{exp}}}{\eta_{\mathrm{W}}}$ was plotted against the atomic number *Z* and the data points were fitted using a second-degree polynomial, as seen in Fig. 1b (for $\eta_{\mathrm{KL}}^{\mathrm{T}}$), Fig. 2b (for $\eta_{\mathrm{KL2}}^{\mathrm{R}}$), Fig. 3b (for $\eta_{\mathrm{KL3}}^{\mathrm{R}}$), and Fig. 4b (for $\eta_{\mathrm{KM}}^{\mathrm{R}}$). (Meddouh *et al*. 2024):

$$S = B_0 + \sum_{i=1}^{2} B_i Z^i = g(Z) \tag{5}$$

The semi-empirical vacancy transfer probabilities can be expressed as follows:

$$\eta_{\mathrm{s-emp}} = f(Z) \times g(Z) \tag{6}$$

Table 1 presents the fitting coefficients for both equations (4) and (5). The semi-empirical values, calculated using equation (6), are presented and organized for $\eta_{\mathrm{KL}}^{\mathrm{T}}$ within the range 16 ≤ *Z* ≤ 92, $\eta_{\mathrm{KL2}}^{\mathrm{R}}$ and $\eta_{\mathrm{KL3}}^{\mathrm{R}}$ within the range 23 ≤ *Z* ≤ 92, and for $\eta_{\mathrm{KM}}^{\mathrm{R}}$ within the range 24 ≤ *Z* ≤ 92, in Tables 2 to 5.

The deviation between the calculated semi-empirical values $\eta_{\mathrm{s-emp}}$ and their corresponding experimental values η_{exp} for vacancy transfer probabilities is quantified by the root-mean-square error ($\varepsilon_{\mathrm{RMS}}$). This measure is computed using the formula (Kahoul *et al*. 2014, 2012, 2011; Sahnoune *et al*. 2020):

$$\varepsilon_{\mathrm{RMS}} = \left[\frac{1}{N}\sum_{j=1}^{N}\left(\frac{\eta_{\mathrm{j-exp}} - \eta_{\mathrm{s-emp}}}{\eta_{\mathrm{s-emp}}}\right)^{2}\right]^{1/2} \quad (7)$$

Here, N represents the total number of experimental data points for each element. The root-mean-square error ($\varepsilon_{\mathrm{RMS}}$) is a frequently used quantity to check the quality and accuracy of the fit and measure the difference between observed (experimental) values and those predicted by a model (semi-empirical). For each element, ($\varepsilon_{\mathrm{RMS}}$) serves as a crucial indicator of the reliability of the semi-empirical model in capturing the experimental data.

The root-mean-square error ($\varepsilon_{\mathrm{RMS}}$) values of the semi-empirical results are shown for $\eta_{\mathrm{KL}}^{\mathrm{T}}$, $\eta_{\mathrm{KL2}}^{\mathrm{R}}$, $\eta_{\mathrm{KL3}}^{\mathrm{R}}$, and $\eta_{\mathrm{KM}}^{\mathrm{R}}$ parameters in Tables 2-5. It should also be noted that as the elements shown in bold in these tables have not yet had their experimental values reported, $\varepsilon_{\mathrm{RMS}}$ values for these elements have not been added

3. Results and discussion

This work presents a comprehensive assessment of semi-empirical vacancy transfer probabilities, including $\eta_{\mathrm{KL}}^{\mathrm{T}}$, $\eta_{\mathrm{KL2}}^{\mathrm{R}}$, $\eta_{\mathrm{KL3}}^{\mathrm{R}}$, and $\eta_{\mathrm{KM}}^{\mathrm{R}}$. Detailed comparisons are provided with theoretical values, fitted outcomes, and experimental data from various sources (Tables 2-5). The root-mean-square error ($\varepsilon_{\mathrm{RMS}}$) for the semi-empirical results is also included in these tables.

To facilitate a thorough evaluation, all vacancy transfer probability values are plotted against the atomic number Z in Fig. 5. The present semi-empirical calculations (derived from formula (6)) demonstrate good agreement with theoretical, fitted, and experimental values across the range $16 \le Z \le 92$ for $\eta_{\mathrm{KL}}^{\mathrm{T}}$, $23 \le Z \le 92$ for $\eta_{\mathrm{KL2}}^{\mathrm{R}}$, and $\eta_{\mathrm{KL3}}^{\mathrm{R}}$, and $24 \le Z \le 92$ for $\eta_{\mathrm{KM}}^{\mathrm{R}}$. Specifically, marginal discrepancies are observed (ranging from 0.04% to 5.51% and 0.22% to 5.25%) for $\eta_{\mathrm{KL}}^{\mathrm{T}}$, When compared to the average experimental values from Rao *et al*. (1972) and the theoretical results from Berkani *et al*. (2025) respectively. However, larger deviations are found for elements $_{88}$Ra, $_{90}$Th, and $_{92}$U when compared with Rao *et al*. (1972) (9.08%, 14.19%, and

21.46%, respectively). These discrepancies are not entirely unexpected for heavy elements, as relativistic effects complicate theoretical predictions. Additionally, the inherent challenges and heterogeneity in experimental measurements for the high-Z elements contribute to these variations, suggesting that these deviations fall within acceptable margins given the complexities involved. Similarly, comparisons with the semi-empirical values of Schönfeld and JanBen (1996) and the empirical values of Berkani *et al*. (2024) reveal variations ranging from 0.01% to 7.54% and 0.1% to 6.31%, respectively. However, for the last five elements, deviations increase to a range of 9.49% to 21.61% compared to Schönfeld and JanBen (1996), while for the last three elements, deviations range from 8.30% to 13.59% when compared to Berkani *et al*. (2024). Encouragingly, the obtained semi-empirical results align closely with the experimental data from Ertuğral *et al*. 2006 (within 0.11% to 2.52%), Öz 2006 (within 0.13% to 0.87%), and Ertuğral *et al.* 2005 (within 0.13% to 1.98%), except for elements $_{90}$Th and $_{92}$U, exhibiting deviations of 11.17% and 17.94%, respectively. These relative differences (RD%) were calculated using the formula $\mathrm{RD\%} = \frac{|\eta - \eta_{\mathrm{s-emp}}|}{\eta_{s-\mathrm{emp}}} \times 100$ (Amari *et al*. 2024b; Zidi *et al*. 2024b). The semi-empirical results (Fig. 5) demonstrate strong alignment with the results of Rao *et al*. (1972), with relative differences ranging from 0.11% to 4.15% except for $_{17}$Cl (which deviates 9.21%) for $\eta^{\mathrm{R}}_{\mathrm{KL2}}$, 0.02% to 1.83% for $\eta^{\mathrm{R}}_{\mathrm{KL3}}$, and 0.28% to 5.41% for $\eta^{\mathrm{R}}_{\mathrm{KM}}$, and of Berkani *et al*. (2025) with relative differences from 0.41% to 3.58% for $\eta^{\mathrm{R}}_{\mathrm{KL2}}$, and 0.08% to 1.15% for $\eta^{\mathrm{R}}_{\mathrm{KL3}}$, excluding elements $_{26}$Fe and $_{30}$Zn, with deviations of 42.15% and 8.57%, respectively. Our comparison with experimental measurements also indicates a good agreement, showing deviations from 0.00% to 2.58%, 0.4% to 3.71%, and 0.12% to 2.04% for Ertuğrul (2002d), 0.32% to 2.28%, 0.09% to 2.45%, and 0.16% to 2.68% for Çalişkan *et al*. (2002), 0.11% to 0.93%, 0.19% to 1.21%, and 0.18% to 2.51% for Durak and Özdemir (1998), and 0.21% to 1.06%, 0.09% to 0.87%, and 0.19% to 1.44% for Ertuğrul *et al*. (1997a). These

deviation values correspond to η^{R}_{KL2}, η^{R}_{KL3}, and η^{R}_{KM}, respectively. Furthermore, excellent agreement is observed with the empirical values reported by Berkani *et al*. (2024)

Figure 6 further reinforces the validity of the approach by illustrating the ε_{RMS} between the semi-empirical calculations and experimental data for η^{T}_{KL}, η^{R}_{KL2}, η^{R}_{KL3}, and η^{R}_{KM}, across various elements. The ε_{RMS} values for most elements reside within a narrow range of 0% to 5%, indicating strong agreement between calculated results and experimental data. However, exceptions exist for certain elements: $_{38}$Sr, $_{41}$Nb, $_{44}$Ru, $_{45}$Rh, $_{46}$Pd, $_{77}$Ir, $_{83}$Bi, $_{90}$Th, and $_{92}$U for η^{T}_{KL}, $_{23}$V, $_{24}$Cr, $_{27}$Co, and $_{28}$Ni for η^{R}_{KL2} and η^{R}_{KL3}, and $_{24}$Cr, $_{28}$Ni, $_{56}$Ba, and $_{66}$Dy for η^{R}_{KM}. As mentioned in a previous paper, these deviations likely stem from data heterogeneity, as values were sourced from diverse references with varying experimental conditions (Berkani *et al*. 2024). Despite these exceptions, the overall consistency of the ε_{RMS} values for most elements support the credibility of the semi-empirical results. Furthermore, the findings exhibit consistency with various theoretical, experimental, empirical, and semi-empirical studies, strengthening their validity.

4. Conclusion

This work presents a novel set of semi-empirical vacancy transfer probabilities η^{T}_{KL}, η^{R}_{KL2}, η^{R}_{KL3}, and η^{R}_{KM}, along with their corresponding fitting coefficients. These probabilities were determined using simple methods for a wide range of elements, covering atomic numbers $16 \leq Z \leq 92$ for η^{T}_{KL}, $24 \leq Z \leq 92$ for η^{R}_{KL2} and η^{R}_{KL3}, and $23 \leq Z \leq 92$ for η^{R}_{KM}. Notably, the results demonstrate relatively good agreement with data from other research groups across the entire atomic range, underscoring the effectiveness of the chosen methodology.

Beyond complementing existing data, the newly obtained semi-empirical vacancy transfer probabilities offer a valuable resource for the scientific and technical community. Their inclusion in atomic databases will provide researchers and professionals with a comprehensive

and up-to-date reference for various applications. Furthermore, this methodology contributes to theoretical atomic physics by refining vacancy transfer parameters, which are essential for improving electron interaction models. The enhanced dataset serves as a reliable benchmark for adjusting theoretical calculations of Auger and radiative transition rates, facilitating more accurate modeling of electron correlation and relativistic effects in heavy elements. These improvements are particularly significant for high-Z elements, where relativistic effects play a dominant role.

Figures captions:

Fig. 1. (a): Distribution of weighted values $\left(\eta_{\mathrm{KL}}^{\mathrm{T}}\right)_{\mathrm{W}}$, The curve is the fitting according to the Eq. (4); (b): distribution of $\frac{\left(\eta_{\mathrm{KL}}^{\mathrm{T}}\right)_{\mathrm{exp}}}{\left(\eta_{\mathrm{KL}}^{\mathrm{T}}\right)_{\mathrm{W}}}$, the curve is the fitting according to Eq. (5), within the range $16 \leq Z \leq 92$ as a function of the atomic number *Z*.

Fig. 2. (a): Distribution of weighted values $\left(\eta_{\mathrm{KL2}}^{\mathrm{R}}\right)_{\mathrm{W}}$, The curve is the fitting according to the Eq. (4); (b): distribution of $\frac{\left(\eta_{\mathrm{KL2}}^{\mathrm{R}}\right)_{\mathrm{exp}}}{\left(\eta_{\mathrm{KL2}}^{\mathrm{R}}\right)_{\mathrm{W}}}$, the curve is the fitting according to Eq. (5), within the range $24 \leq Z \leq 92$ as a function of the atomic number *Z*.

Fig. 3. (a): Distribution of weighted values $\left(\eta_{\mathrm{KL3}}^{\mathrm{R}}\right)_{\mathrm{W}}$, , the curve is the fitting according to the Eq. (4); (b): distribution of $\frac{\left(\eta_{\mathrm{KL3}}^{\mathrm{R}}\right)_{\mathrm{exp}}}{\left(\eta_{\mathrm{KL3}}^{\mathrm{R}}\right)_{\mathrm{W}}}$, the curve is the fitting according to Eq. (5), within the range $24 \leq Z \leq 92$ as a function of the atomic number *Z*.

Fig. 4. (a): Distribution of weighted values $\left(\eta_{\mathrm{KM}}^{\mathrm{R}}\right)_{\mathrm{W}}$, , the curve is the fitting according to Eq. (4), (b): distribution of $\frac{\left(\eta_{\mathrm{KM}}^{\mathrm{R}}\right)_{\mathrm{exp}}}{\left(\eta_{\mathrm{KM}}^{\mathrm{R}}\right)_{\mathrm{W}}}$, the curve is the fitting according to Eq. (5) (Fig. 1b), within the range $23 \leq Z \leq 92$ as a function of the atomic number *Z*.

Fig. 5. Comparison of current semi-empirical vacancy transfer probabilities with theoretical, fitted, and experimental values for $\eta_{\mathrm{KL}}^{\mathrm{T}}$, $\eta_{\mathrm{KL2}}^{\mathrm{R}}$, $\eta_{\mathrm{KL3}}^{\mathrm{R}}$, and $\eta_{\mathrm{KM}}^{\mathrm{R}}$ as a function of atomic number *Z*.

Fig. 6. Root-mean-square error ($\varepsilon_{\mathrm{RMS}}$) for $\eta_{\mathrm{KL}}^{\mathrm{T}}$, $\eta_{\mathrm{KL2}}^{\mathrm{R}}$, $\eta_{\mathrm{KL3}}^{\mathrm{R}}$, and $\eta_{\mathrm{KM}}^{\mathrm{R}}$as a function of atomic number *Z*.

References:

Akman, F., 2016a. K to L shell vacancy transfer probabilities and Auger electron emission ratios for elements in the atomic range 30≤Z≤58. Can. J. Phys. 94, 679–686. https://doi.org/10.1139/cjp-2016-0097

Akman, F., 2016b. Experimental values of K to Li sub-shell, K to L, and K to M shell vacancy transfer probabilities for some rare earth elements. Applied Radiation and Isotopes 115, 295–303. https://doi.org/10.1016/j.apradiso.2016.07.014

Alım, B., Uğurlu, M., Han, İ., Demir, L., 2017a. Determination of K shell XRF parameters and K to L shell vacancy transfer probabilities of ferromagnetic 3d transition metals. Presented at the II. INTERNATIONAL CONFERENCE ON ADVANCES IN NATURAL AND APPLIED SCIENCES: ICANAS 2017, Antalya, Turkey, p. 020085. https://doi.org/10.1063/1.4981733

Alım, B., Uğurlu, M., Han, İ., Demir, L., 2017b. Investigation of alloying effects on XRF parameters of 3d transition metals in Permendur49, Kovar and Ti50Co50 alloys. Journal of Radiation Research and Applied Sciences 11, 144–149. https://doi.org/10.1016/j.jrras.2017.12.003

Amari, K., Kahoul, A., Sampaio, J.M., Daoudi, S., Marques, J.P., Parente, F., Hamidani, A., Croft, S., Favalli, A., Kasri, Y., Zidi, A., Berkani, B., 2024a. Experimental K-shell fluorescence cross sections for elements in the atomic number range $16 \leq Z \leq 92$ by photon impact at various energies. Atomic Data and Nuclear Data Tables 159, 101662. https://doi.org/10.1016/j.adt.2024.101662

Amari, K., Kahoul, A., Sampaio, J.M., Kasri, Y., Marques, J.P., Parente, F., Hamidani, A., Croft, S., Favalli, A., Daoudi, S., Deghfel, B., Zidi, A., Berkani, B., 2024b. Empirical calculation of K-shell fluorescence cross sections for elements in the atomic range $16 \leq Z \leq 92$ by photon effects ranging from 5.46 to 123.6 keV (Three-dimensional formulae). Phys. Scr. 99, 105402. https://doi.org/10.1088/1402-4896/ad720e

Anand, L.F.M., Gudennavar, S.B., Bubbly, S.G., Kerur, B.R., 2018. K-Shell X-Ray Fluorescence Parameters of a Few Low Z Elements. J. Exp. Theor. Phys. 126, 1–7. https://doi.org/10.1134/S1063776118010016

Anand, L.F.M., Gudennavar, S.B., Bubbly, S.G., Kerur, B.R., 2015. Kβ to Kα X-ray intensity ratios and K to L shell vacancy transfer probabilities of Co, Ni, Cu, and Zn. J. Exp. Theor. Phys. 121, 961–965. https://doi.org/10.1134/S1063776115130087

Anand, L.F.M., Gudennavar, S.B., Bubbly, S.G., Kerur, B.R., 2014. K-shell X-ray intensity ratios and vacancy transfer probabilities of Pt, Au, and Pb by a simple method. J. Exp. Theor. Phys. 119, 392–397. https://doi.org/10.1134/S1063776114090076

Anand, L.F.M., Gudennavar, S.B., Joseph, D., G. Bubbly, S., 2013. K_β to K_α Intensity Ratio and Total Vacancy Transfer Probabilities of Molybdenum and Silver. ujpa 7, 83–87. https://doi.org/10.13189/ujpa.2013.010205

Anand, L.F.M., Rameshan, M.T., Gudennavar, S.B., Bubbly, S.G., Horakeri, L.D., Kerur, B.R., 2012. Vacancy Transfer Probability Of Platinum And Lead By Using 2π-Geometrical Configuration And A Weak γ- Source. Conference: Proceedings of the 19th NSRP 1.

Apaydın, G., Tıraşoğlu, E., 2012. Calculation of vacancy transfer probabilities from K to L shell using the X-ray fluorescence parameters. Radiation Physics and Chemistry 81, 1593–1594. https://doi.org/10.1016/j.radphyschem.2012.04.002

Aylikci, V., Kahoul, A., Aylikci, N.K., Tiraşoğlu, E., Karahan, İ.H., 2015. Empirical, Semi-Empirical and Experimental Determination of K X-Ray Fluorescence Parameters of Some Elements in the Atomic Range $21 \leq Z \leq 30$. Spectroscopy Letters 48, 331–342. https://doi.org/10.1080/00387010.2014.881381

Bambynek, W., Crasemann, B., Fink, R.W., Freund, H.-U., Mark, H., Swift, C.D., Price, R.E., Rao, P.V., 1972. X-Ray Fluorescence Yields, Auger, and Coster-Kronig Transition Probabilities. Rev. Mod. Phys. 44, 716–813. https://doi.org/10.1103/RevModPhys.44.716

Baydaş, E., 2005. Determination of Ratios of Emission Probabilities of Auger Electrons and K to L Shell Radiative Vacancy Transfer Probabilities for 16 Elements from Ag to Er at 59.5 keV. Instrumentation Science & Technology 33, 461–471. https://doi.org/10.1081/CI-200063723

Bennal, A.S., Badiger, N.M., 2006. Measurement of K–L radiative vacancy transfer probabilities for Ta, Au and Pb in a 2π geometrical configuration. Nuclear Instruments and Methods in Physics Research Section B: Beam Interactions with Materials and Atoms 247, 161–165. https://doi.org/10.1016/j.nimb.2006.01.057

Bennal, A.S., Niranjan, K.M., Badiger, N.M., 2010. Determination of K to L shell total vacancy transfer probabilities using a weak gamma source: An alternative method. Journal of Quantitative Spectroscopy and Radiative Transfer 111, 1363–1371. https://doi.org/10.1016/j.jqsrt.2010.02.012

Berkani, B., Kahoul, A., Sampaio, J.M., Daoudi, S., Marques, J.P., Parente, F., Hamidani, A., Croft, S., Favalli, A., Kasri, Y., Zidi, A., Amari, K., 2025. Relativistic and semi-theoretical calculations of K-shell to L-shell/subshell vacancy transfer probabilities. Spectrochimica Acta Part B: Atomic Spectroscopy 224, 107089. https://doi.org/10.1016/j.sab.2024.107089

Berkani, B., Kahoul, A., Sampaio, J.M., Daoudi, S., Marques, J.P., Parente, F., Hamidani, A., Croft, S., Favalli, A., Kasri, Y., Zidi, A., Amari, K., 2024. Vacancy transfer probability parameters: Database and a new empirical value for elements in the atomic number range $16 \leq Z \leq 92$. Radiation Physics and Chemistry 225, 112106. https://doi.org/10.1016/j.radphyschem.2024.112106

Çalişkan, B., ErtugÄrul, M., Oz, E., ErdogÄan, H., 2002. Measurement of radiative vacancy distributions for the L2; L3 subshell and M shell of some elements with atomic range $41 \leq Z \leq 68$. https://doi.org/10.1016/S0022-4073(01)00192-3

Cengiz, E., Aylıkcı, V., Kaya, N., Apaydın, G., Tıraşoğlu, E., 2008. Chemical effects on K and L shell production cross sections and transfer probabilities in Nb compounds. J Radioanal Nucl Chem 278, 89–96. https://doi.org/10.1007/s10967-007-7202-3

Cengiz, E., Tıraşoğlu, E., Apaydın, G., Aylıkcı, V., Küp Aylıkcı, N., Aksoy, C., 2011. K-shell X-ray fluorescence parameters of some heavy elements and compounds. Radiation Physics and Chemistry 80, 328–334. https://doi.org/10.1016/j.radphyschem.2010.09.008

Cengiz, E., Tıraşoğlu, E., Aylıkcı, V., Apaydın, G., 2010. The investigations on K and L X-ray fluorescence parameters of gold compounds. Radiation Physics and Chemistry 79, 809–815. https://doi.org/10.1016/j.radphyschem.2010.03.003

Chen, M.H., Crasemann, B., Mark, H., 1979. Relativistic radiationless transition probabilities for atomic K- and L-shells. Atomic Data and Nuclear Data Tables 24, 13–37. https://doi.org/10.1016/0092-640X(79)90037-8

Daoudi, S., Kahoul, A., Kup Aylikci, N., Sampaio, J.M., Marques, J.P., Aylikci, V., Sahnoune, Y., Kasri, Y., Deghfel, B., 2020. Review of experimental photon-induced K β /K α intensity ratios. Atomic Data and Nuclear Data Tables 132, 101308. https://doi.org/10.1016/j.adt.2019.101308

Demir, D., Şahin, Y., 2007. Measurements of K-shell x-ray production cross sections and K to L and M-shell radiative vacancy transfer probabilities for Nd, Eu, Gd, Dy and Ho at excitation with 59.5 keV photons in an external magnetic field. X-Ray Spectrometry 36, 178–184. https://doi.org/10.1002/xrs.941

Durak, R., Özdemir, Y., 2000. Measurement of K- to L- and M-shell radiative vacancy transfer probabilities in lanthanide elements by 59.54 keV photons. X-Ray Spectrom. 29, 151–154. https://doi.org/10.1002/(SICI)1097-4539(200003/04)29:2<151::AID-XRS402>3.0.CO;2-Z

Durak, R., Özdemir, Y., 1998. K- to L- and M-shell radiative vacancy transfer probability measurements in some elements from Nd to Pb. J. Phys. B: At. Mol. Opt. Phys. 31, 3575–3581. https://doi.org/10.1088/0953-4075/31/16/011

Durak, R., Turhan, M.F., Sağlam, M., Ateş, A., 2012. Measurements of Radiative Vacancy Transfer Probabilities for Some Elements Irradiated with Photons of 0.0208 Nanometer Wavelengths. International Conference Nanomaterials: Applications and Properties 1, 04RES10(2pp).

Durdu, B.G., Akkutlu, E., Küçükönder, A., Çam, H., 2022. Analytical Investigation on Some K X-Ray Fluorescence Parameters of Barium Compounds. Acta Phys. Pol. A 141, 474–480. https://doi.org/10.12693/APhysPolA.141.474

Ertuğral, B., Apaydin, G., Baltas, H., Çevik, U., Kobya, A.İ., Ertuğrul, M., 2005. Measurement of vacancy transfer probabilities from K to L shell for high atomic number elements. Spectrochimica Acta Part B: Atomic Spectroscopy 60, 519–524. https://doi.org/10.1016/j.sab.2005.03.009

Ertuğral, B., Apaydın, G., Tekbıyık, A., Tıraşoğlu, E., Çevik, U., Kobya, A.İ., Ertuğrul, M., 2006. Determination of probabilities of vacancy transfer from K to L shell using K X-ray intensity ratios. Eur. Phys. J. D 37, 371–375. https://doi.org/10.1140/epjd/e2005-00326-y

Ertuğral, B., Baltaş, H., Çelik, A., Kobya, Y., 2010. Vacancy Transfer Probabilities from K to L Shell for Low Atomic Number Elements at 5.96 keV. Acta Phys. Pol. A 117, 900–903. https://doi.org/10.12693/APhysPolA.117.900

Ertuğral, B., Cevik, U., Tirasoglu, E., Kopya, A.I., Ertugrul, M., Dogan, O., 2003. Measurement of K to L shell vacancy transfer probabilities for the elements 52⩽Z⩽68. Journal of Quantitative Spectroscopy and Radiative Transfer 78, 163–169. https://doi.org/10.1016/S0022-4073(02)00189-9

Ertuğrul, M., 2003. Determination of probabilities of vacancy transfer from the K to the Li subshell using L x-ray production cross-sections. J. Phys. B: At. Mol. Opt. Phys. 36, 2275–2282. https://doi.org/10.1088/0953-4075/36/11/312

Ertuğrul, M., 2002a. Measurement of total, radiative and radiationless (Auger) vacancy transfer probabilities from K to L i (i=1, 2, 3) subshell of Ho and Er. Spectrochimica Acta Part B: Atomic Spectroscopy 57, 63–71. https://doi.org/10.1016/S0584-8547(01)00352-4

Ertuğrul, M., 2002b. Measurement of total, radiative and radiationless (Auger) vacancy transfer probabilities from K to Li subshell of Sm and Tb. Journal of Radioanalytical and Nuclear Chemistry 252, 545–550. https://doi.org/10.1023/a:1015811022240

Ertuğrul, M., 2002c. Measurement of total, radiative and radiationless (Auger) vacancy transfer probabilities from K to Li sub-shells of Cs, Ba and La. J. Anal. At. Spectrom. 17, 64–68. https://doi.org/10.1039/b103366m

Ertuğrul, M., 2002d. Measurement of K shell radiative transition probabilities and K, L2 and L3 shell/subshell fluorescence yields of some elements in the atomic number range 30 ≤ Z ≤ 40. Analytica Chimica Acta 454, 327–334. https://doi.org/10.1016/S0003-2670(01)01554-9

Ertuğrul, M., Doğan, O., Şimşek, Ö., 1997a. Measurement of radiative vacancy distributions for the L2, L3 subshell and M shell of some elements with atomic range 69≤Z≤92. Radiation Physics and Chemistry 49, 221–224. https://doi.org/10.1016/0969-806X(95)00459-B

Ertuğrul, M., Doğan, O., Şimşek, Ö., Turgut, Ü., Erdŏgan, H., 1997b. Measurement of probabilities for vacancy transfer from the K to L shell of the elements 73⩽Z⩽92. Phys. Rev. A 55, 303–306. https://doi.org/10.1103/PhysRevA.55.303

George, L., Gudennavar, S.B., Joseph, D., Bubbly, S.G., 2014. K shell X-ray intensity ratios and vacancy transfer probabilities of Fe, Ag, and Te following electron capture decay. Can. J. Phys. 92, 1301–1304. https://doi.org/10.1139/cjp-2013-0697

Gudennavar, S.B., Bubbly, S.G., 2023. Kβ to Kα X-ray intensity ratio and K–L vacancy transfer probability of Mn following electron capture decay. Can. J. Phys. cjp-2023-0080. https://doi.org/10.1139/cjp-2023-0080

Hamidani, A., Daoudi, S., Kahoul, A., Sampaio, J.M., Marques, J.P., Parente, F., Croft, S., Favalli, A., Kup Aylikci, N., Aylikci, V., Kasri, Y., Meddouh, K., 2023. Updated database, semi-empirical and theoretical calculation of K β /K α intensity ratios for elements ranging from 11 Na to 96 Cm. Atomic Data and Nuclear Data Tables 149, 101549. https://doi.org/10.1016/j.adt.2022.101549

Han, I., Demir, L., 2010. Alloying effect on K to L shell vacancy transfer probabilities in 3d transition metals. Radiation Physics and Chemistry 79, 1174–1179. https://doi.org/10.1016/j.radphyschem.2010.07.015

Han, I., Demir, L., Ağbaba, M., 2007. Measurements of L X-ray production cross sections, L subshell fluorescence yields and K to L shell vacancy transfer probabilities. Radiation Physics and Chemistry 76, 1551–1559. https://doi.org/10.1016/j.radphyschem.2007.04.006

Kahoul, A., Abassi, A., Deghfel, B., Nekkab, M., 2011. K-shell fluorescence yields for elements with 6≤Z≤99. Radiation Physics and Chemistry 80, 369–377. https://doi.org/10.1016/j.radphyschem.2010.11.011

Kahoul, A., Aylikci, V., Aylikci, N.K., Cengiz, E., Apaydın, G., 2012. Updated database and new empirical values for K-shell fluorescence yields. Radiation Physics and Chemistry 81, 713–727. https://doi.org/10.1016/j.radphyschem.2012.03.006

Kahoul, A., Aylikci, V., Deghfel, B., Küp Aylikci, N., Nekkab, M., 2014. New empirical formulae for calculation of average M-shell fluorescence yields. Journal of Quantitative Spectroscopy and Radiative Transfer 145, 205–213. https://doi.org/10.1016/j.jqsrt.2014.05.009

Kaya, S., Karabıdak, S.M., Çevik, U., 2014. K-L Vacancy Transfer Probabilities For Some Pure Metals In The Atomic Range 24≤Z≤56 Usıng 59 5 Kev Photons. Batman University Journal of Life Sciences 4, 66–76.

Meddouh, K., Kahoul, A., Sampaio, J.M., Daoudi, S., Marques, J.P., Parente, F., Aylikci, N.K., Aylikci, V., Kasri, Y., Hamidani, A., 2024. Semi-Empirical and Theoretical Calculation of 1, 2, and 3 Subshell Fluorescence Yields. Journal of Quantitative Spectroscopy and Radiative Transfer 322, 109013. https://doi.org/10.1016/j.jqsrt.2024.109013

Mirji, S., Bennal, A.S., Badiger, N.M., Tiwari, M.K., Lodha, G.S., 2015a. Chemical sensitivity of K-L vacancy transfer probability in compounds of 3d atoms using synchrotron radiation. Chemical Physics Letters 634, 271–276. https://doi.org/10.1016/j.cplett.2015.06.012

Mirji, S., Bennal, A.S., Krishnananda, Badiger, N.M., Tiwari, M.K., Lodha, G.S., 2015b. Determination of K–L vacancy transfer probabilities of some 3d elements using synchrotron radiation. Can. J. Phys. 93, 760–764. https://doi.org/10.1139/cjp-2014-0552

Onder, P., Tursucu, A., Demir, D., 2013. K Shell X-Ray Fluorescence Parameters of Some Elements in the Atomic Range. Science and Technology of Nuclear Installations 2013, 1–6. https://doi.org/10.1155/2013/285190

Öz, E., 2006. Determination of ratios of emission probabilities of Auger electrons and K–L-shell radiative vacancy transfer probabilities for 17 elements from Mn to Mo at 59.5keV. Journal of Quantitative Spectroscopy and Radiative Transfer 97, 41–50. https://doi.org/10.1016/j.jqsrt.2004.12.016

Puri, S, Mehta, D., Chand, B., Singh, N., Hubbell, J.H., Trehan, P.N., 1993. Production of L, subshell and M shell vacancies following inner-shell vacancy production. Nuclear Instruments and Methods in Physics Research B 83, 21–30. https://doi.org/10.1016/0168-583X(93)95902-H

Puri, S., Mehta, D., Chand, B., Singh, N., Trehan, P.N., 1993. Measurements of K to L shell vacancy transfer probability for the elements $37 \leq Z \leq 42$. Nuclear Instruments and Methods in Physics Research Section B: Beam Interactions with Materials and Atoms 73, 443–446. https://doi.org/10.1016/0168-583X(93)95826-Q

Rao, P.V., Chen, M.H., Crasemann, B., 1972. Atomic Vacancy Distributions Produced by Inner-Shell Ionization. Phys. Rev. A 5, 997–1012. https://doi.org/10.1103/PhysRevA.5.997

Reyes-Herrera, J., Miranda, J., 2009. Measurement of K-L Radiative Vacancy Transfer Probabilities in Rare Earth Elements Bombarded with [sup 12]C and [sup 16]O Ions, in: AIP Conference Proceedings. Presented at the APPLICATION OF ACCELERATORS IN RESEARCH AND INDUSTRY: Twentieth International Conference, AIP, Fort Worth (Texas), pp. 274–277. https://doi.org/10.1063/1.3120031

Reyes-Herrera, J., Miranda, J., 2008. Measurement of K–L radiative vacancy transfer probabilities in selected rare earth elements bombarded with 3–4MeV protons. Nuclear Instruments and Methods in Physics Research Section B: Beam Interactions with Materials and Atoms 266, 5075–5079. https://doi.org/10.1016/j.nimb.2008.09.015

Sahnoune, Y., Kahoul, A., Daoudi, S., Sampaio, J.M., Aylikci, N.K., Aylikci, V., Kasri, Y., Deghfel, B., Marques, J.P., Medjadi, D.E., 2020. Updated database, new empirical and theoretical values of average L shell fluorescence yields of elements with $23 \leq Z \leq 96$. Radiation Physics and Chemistry 166, 108495. https://doi.org/10.1016/j.radphyschem.2019.108495

Sampaio, J.M., Guerra, M., Parente, F., Madeira, T.I., Indelicato, P., Santos, J.P., Marques, J.P., 2016. Calculations of photo-induced X-ray production cross-sections in the energy range 1–150 keV and average fluorescence yields for Zn, Cd and Hg. Atomic Data and Nuclear Data Tables 111–112, 67–86. https://doi.org/10.1016/j.adt.2016.02.001

Santra, S., Mandal, A.C., Mitra, D., Sarkar, M., Bhattacharya, D., 2005. Measurement of the K to L shell vacancy transfer probabilities for Mo, Pd and Cd in photon impact. Radiation Physics and Chemistry 74, 282–287. https://doi.org/10.1016/j.radphyschem.2005.05.010

Schönfeld, E., JanBen, H., 1996. Evaluation of atomic shell data. Nuclear Instruments and Methodsin PhysicsResearchA 369, 527–533.

Scofield, J.H., 1974. Relativistic hartree-slater values for K and L X-ray emission rates. Atomic Data and Nuclear Data Tables 14, 121–137. https://doi.org/10.1016/S0092-640X(74)80019-7

Şimşek, Ö., Karagöz, D., Ertugrul, M., 2003. Measurement of K to L shell vacancy transfer probabilities for the elements $46 \leq Z \leq 55$ by photoionization. Spectrochimica Acta Part B: Atomic Spectroscopy 58, 1859–1865. https://doi.org/10.1016/S0584-8547(03)00158-7

Söğüt, Ö., 2009. Investigation of *K* to *L* shell/subshell vacancy transitions of Zn and Fe in Fe $_x$ Zn $_{1-x}$ thin film alloys. Radiochimica Acta 97, 695–699. https://doi.org/10.1524/ract.2009.1662

Söğüt, Ö., 2006. Measurement of η_{KL} and η_{KM} vacancy transfer in Cr $_x$ Ni $_{1-x}$ and Cr $_x$ Al $_{1-x}$ alloys. Phys. Scr. 73, 466–470. https://doi.org/10.1088/0031-8949/73/5/009

Söğüt, Ö., Büyükkasap, E., Küçükönder, A., Tarakçioğlu, T., 2009. Measurement of vacancy transfer probability from K to L shell using K-shell fluorescence yields. Pramana - J Phys 73, 711–718. https://doi.org/10.1007/s12043-009-0139-z

Sreevidya, P.V., Gudennavar, S.B., Joseph, D., Bubbly, S.G., 2014. K shell X-ray intensity ratios, K-Li, K-L, and K-M vacancy transfer probabilities of Ba and Tl following internal conversion process. Can. J. Phys. 92, 1489–1493. https://doi.org/10.1139/cjp-2014-0105

Turhan, M.F., Akman, F., 2023. K shell fluorescence parameters of some elements at 59.54 keV: Experimental and theoretical results. Nuclear Instruments and Methods in Physics Research Section B: Beam Interactions with Materials and Atoms 534, 16–25. https://doi.org/10.1016/j.nimb.2022.11.003

Turhan, M.F., Akman, F., Kaçal, M.R., Durak, R., 2017. Measurements of K X-ray fluorescence cross-sections, fluorescence yields, level widths and radiative vacancy transition probabilities for the elements Zr, Mo, Cd, Er at 59.54 keV. IOP Conf. Ser.: Mater. Sci. Eng. 282, 012015. https://doi.org/10.1088/1757-899X/282/1/012015

Turhan, M.F., Turşucu, A., Akman, F., Akdemir, F., Durak, R., 2020. Chemical effect on K shell X-ray fluorescence parameters for some Mn and Ni compounds. Radiation Physics and Chemistry 168, 108564. https://doi.org/10.1016/j.radphyschem.2019.108564

Turşucu, A., Demir, D., 2013. Chemical effect on the K shell x-ray fluorescence parameters of some Ce compounds. Applied Radiation and Isotopes 77, 23–26. https://doi.org/10.1016/j.apradiso.2013.02.017

Turşucu, A., Onder, P., Demir, D., 2013. Measurement of Kβ/Kα x-ray intensity ratios and K to L shell total vacancy transfer probabilities for elements in the range $40 \leq Z \leq 50$. Int. J. Phys. Sci. 8, 103–108. https://doi.org/10.5897/IJPS2012.0008

Turşucu, A., Önder, P., Eroğlu, M., Demir, D., 2012. Determination of K–L total vacancy transfer probabilities using a weak gamma source in 2π geometrical configuration. Applied Radiation and Isotopes 70, 1509–1511. https://doi.org/10.1016/j.apradiso.2012.04.029

Uğurlu, M., Akkuş, T., Demir, L., 2020. The magnetic field effect of K X-ray fluorescence parameters of elements in the range $39 \leq Z \leq 48$. Can. J. Phys. 98, 217–221. https://doi.org/10.1139/cjp-2019-0296

Uğurlu, M., Demir, L., 2020. *K* X-ray fluorescence parameters of some fourth period elements in a magnetic field. Spectroscopy Letters 53, 163–171. https://doi.org/10.1080/00387010.2020.1715440

Zidi, A., Kahoul, A., Marques, J.P., Daoudi, S., Sampaio, J.M., Parente, F., Hamidani, A., Croft, S., Favalli, A., Kasri, Y., Amari, K., Berkani, B., 2024a. Databases of L-shell X-ray intensity ratios for various elements after photon excitation. Atomic Data and Nuclear Data Tables 157, 101645. https://doi.org/10.1016/j.adt.2024.101645

Zidi, A., Kahoul, A., Marques, J.P., Daoudi, S., Sampaio, J.M., Parente, F., Hamidani, A., Croft, S., Favalli, A., Kasri, Y., Amari, K., Berkani, B., 2024b. Investigating empirical and theoretical calculations for intensity ratios of L-Shell X-ray transitions in atoms with $39 \leq Z \leq 94$. Journal of Electron Spectroscopy and Related Phenomena 275, 147473. https://doi.org/10.1016/j.elspec.2024.147473

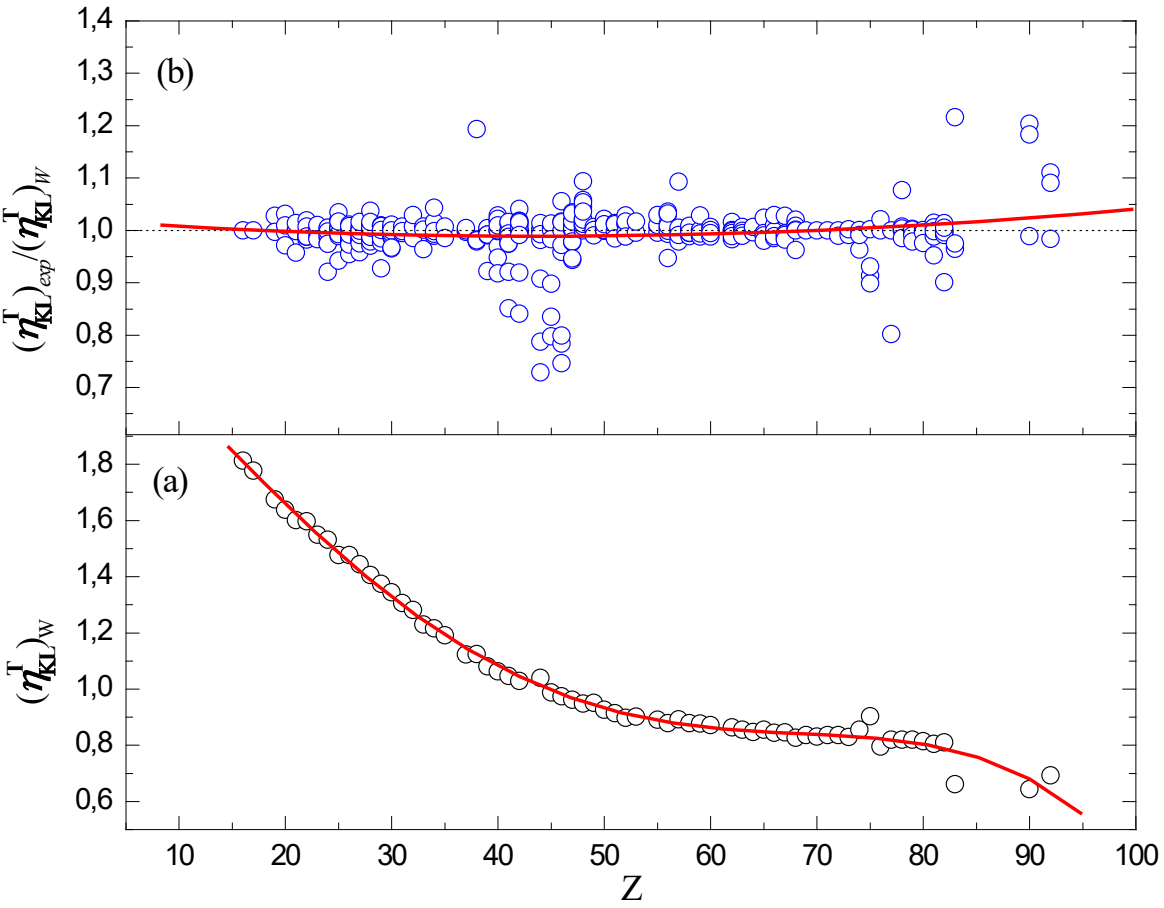
(b)
(a)
$(\eta^T_{Kl})_{exp}/(\eta^T_{Kl})_W$
$(\eta^T_{Kl})_W$
Z
1,4
1,3
1,2
1,1
1,0
0,9
0,8
0,7
1,8
1,6
1,4
1,2
1,0
0,8
0,6
10
20
30
40
50
60
70
80
90
100

Fig. 1

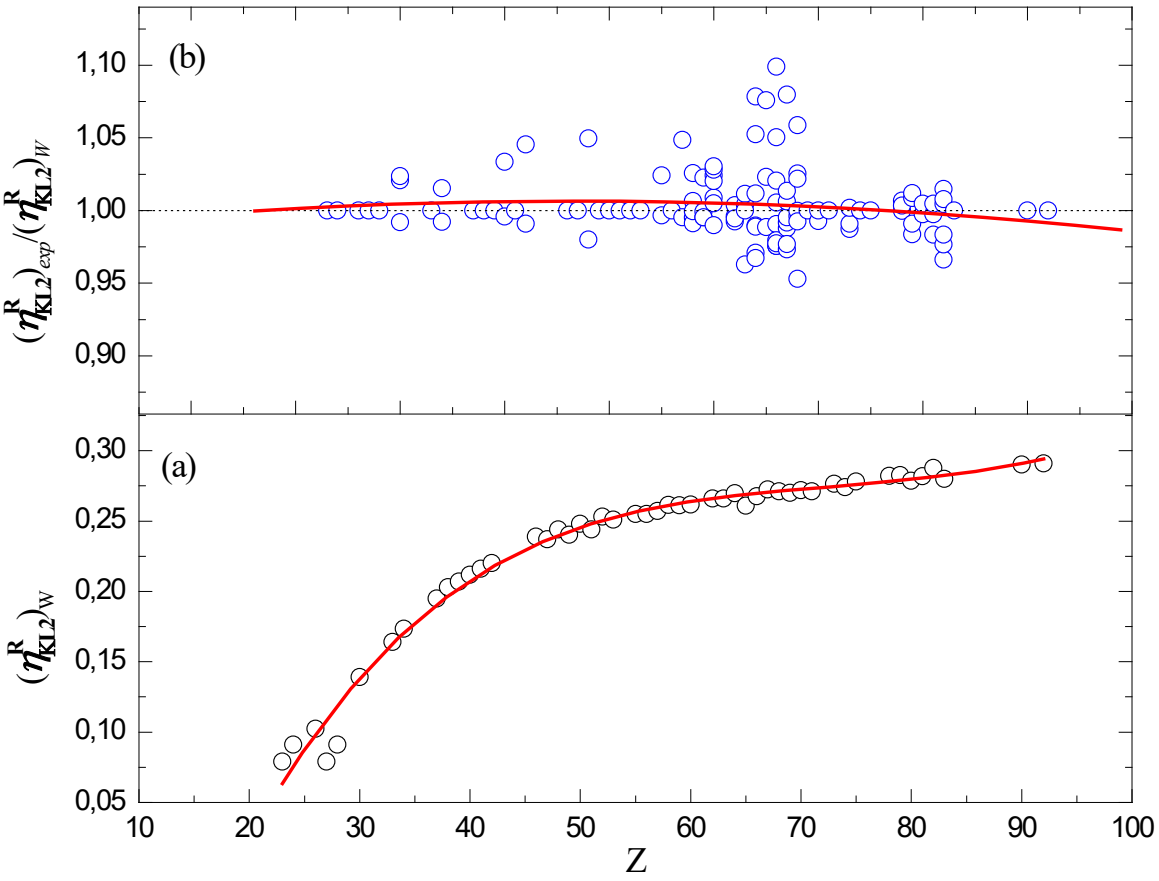
(b)
(a)
$(\eta^R_{Kl2})_{exp}/(\eta^R_{Kl2})_W$
$(\eta^R_{Kl2})_W$
Z
1,10
1,05
1,00
0,95
0,90
0,30
0,25
0,20
0,15
0,10
0,05
10
20
30
40
50
60
70
80
90
100

Fig. 2

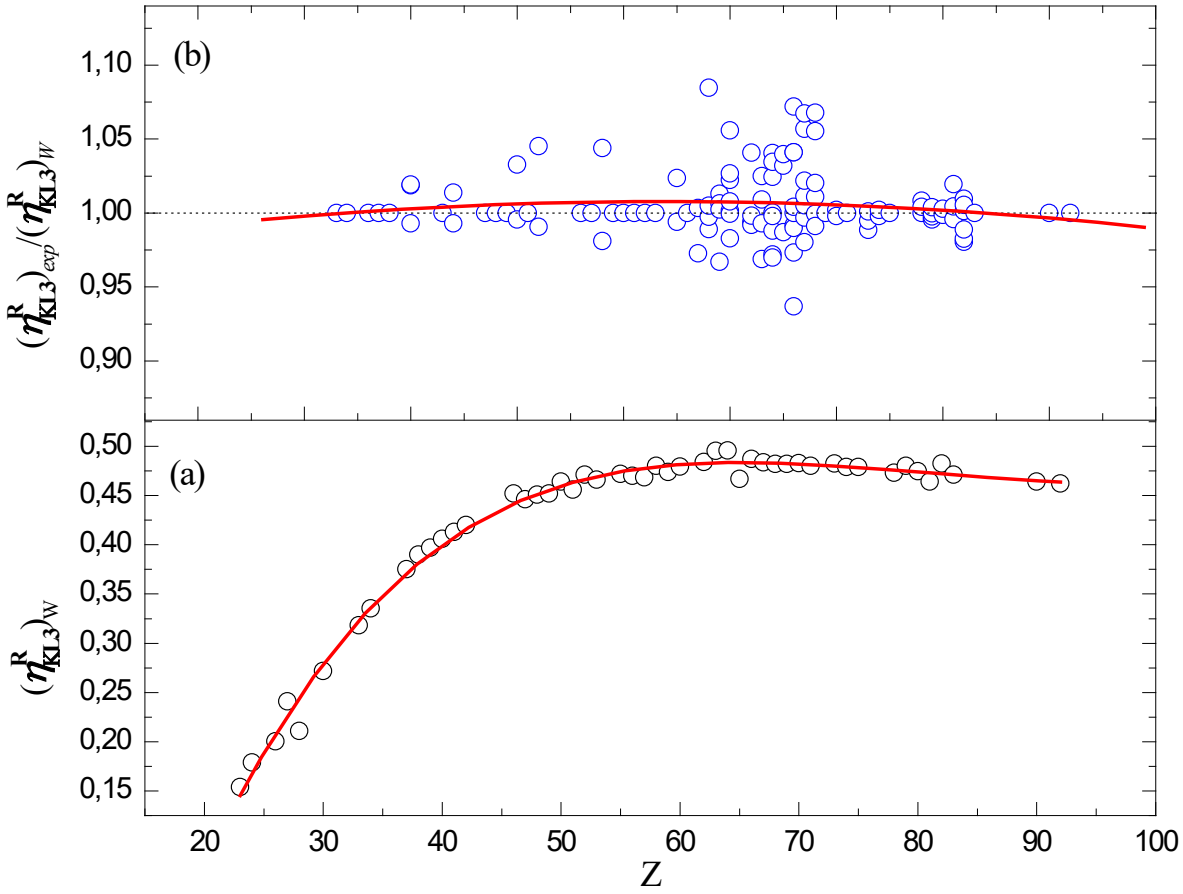
(b)
(a)
$(\eta^R_{K1.3})_{exp}/(\eta^R_{K1.3})_W$
$(\eta^R_{K1.3})_W$
Z
1,10
1,05
1,00
0,95
0,90
0,50
0,45
0,40
0,35
0,30
0,25
0,20
0,15
20
30
40
50
60
70
80
90
100

Fig. 3

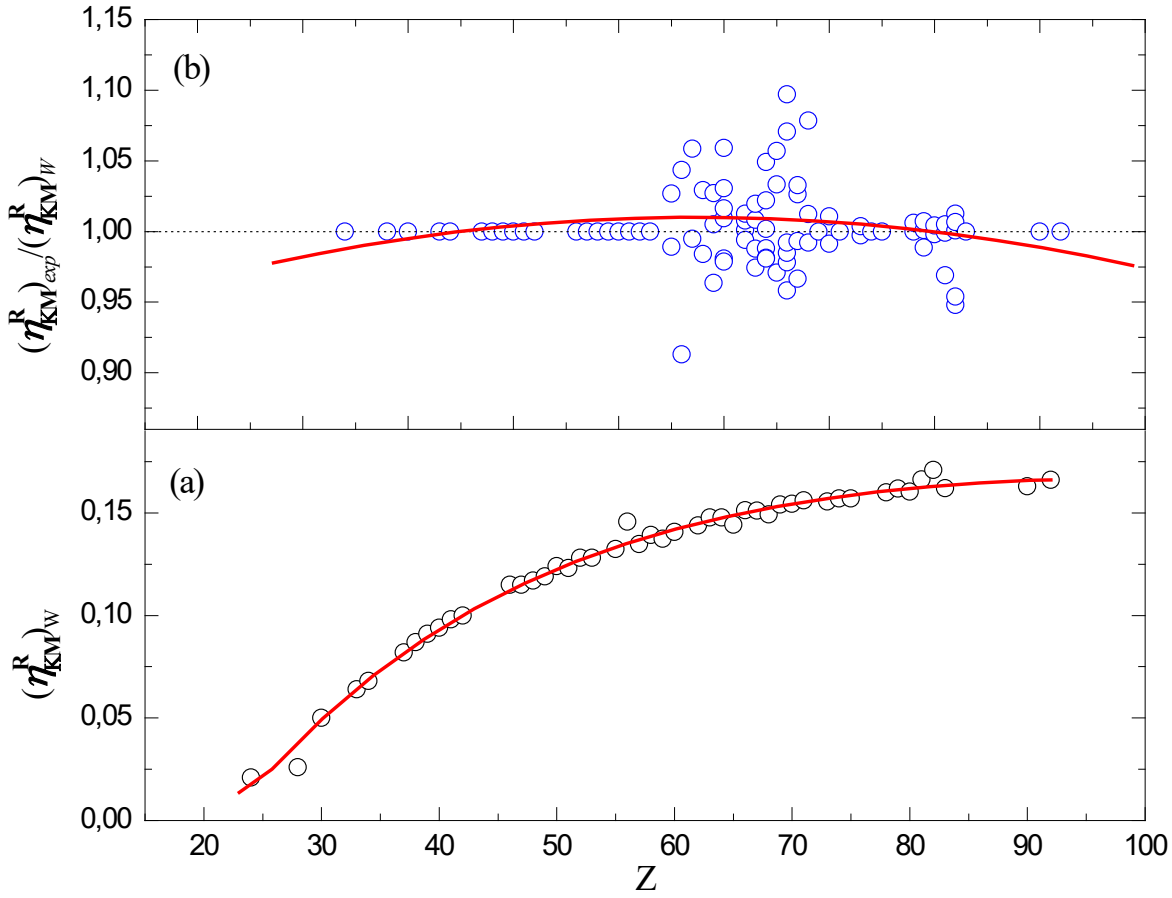
(b)
(a)
$(\eta^R_{KM})_{exp}/(\eta^R_{KM})_W$
$(\eta^R_{KM})_W$
Z
1,15
1,10
1,05
1,00
0,95
0,90
0,15
0,10
0,05
0,00
20
30
40
50
60
70
80
90
100

Fig. 4

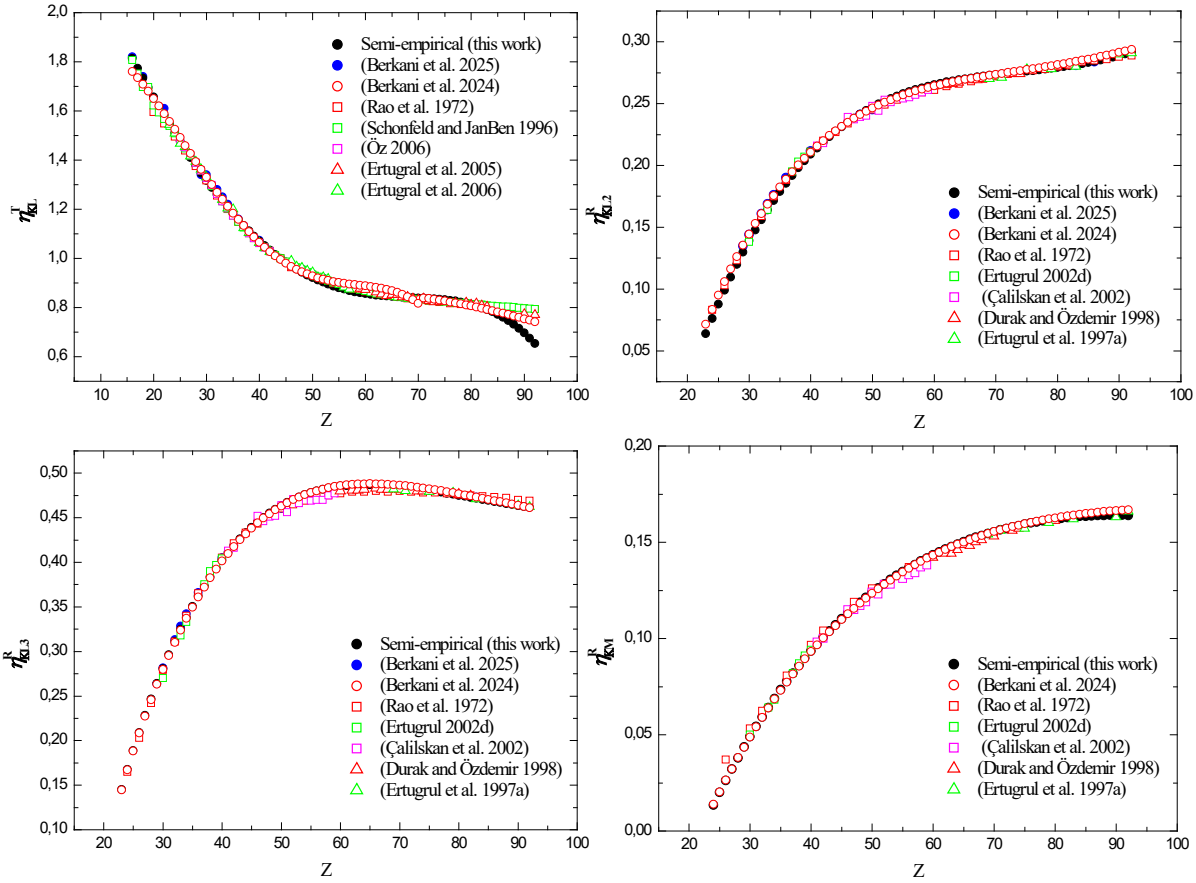
Semi-empirical (this work)
(Berkani et al. 2025)
(Berkani et al. 2024)
(Rao et al. 1972)
(Schonfeld and JanBen 1996)
(Öz 2006)
(Ertugral et al. 2005)
(Ertugral et al. 2006)
Z
Semi-empirical (this work)
(Berkani et al. 2025)
(Berkani et al. 2024)
(Rao et al. 1972)
(Ertugrul 2002d)
(Çalilskan et al. 2002)
(Durak and Özdemir 1998)
(Ertugrul et al. 1997a)
Z
Semi-empirical (this work)
(Berkani et al. 2025)
(Berkani et al. 2024)
(Rao et al. 1972)
(Ertugrul 2002d)
(Çalilskan et al. 2002)
(Durak and Özdemir 1998)
(Ertugrul et al. 1997a)
Z
Semi-empirical (this work)
(Berkani et al. 2024)
(Rao et al. 1972)
(Ertugrul 2002d)
(Çalilskan et al. 2002)
(Durak and Özdemir 1998)
(Ertugrul et al. 1997a)
Z

Fig. 5

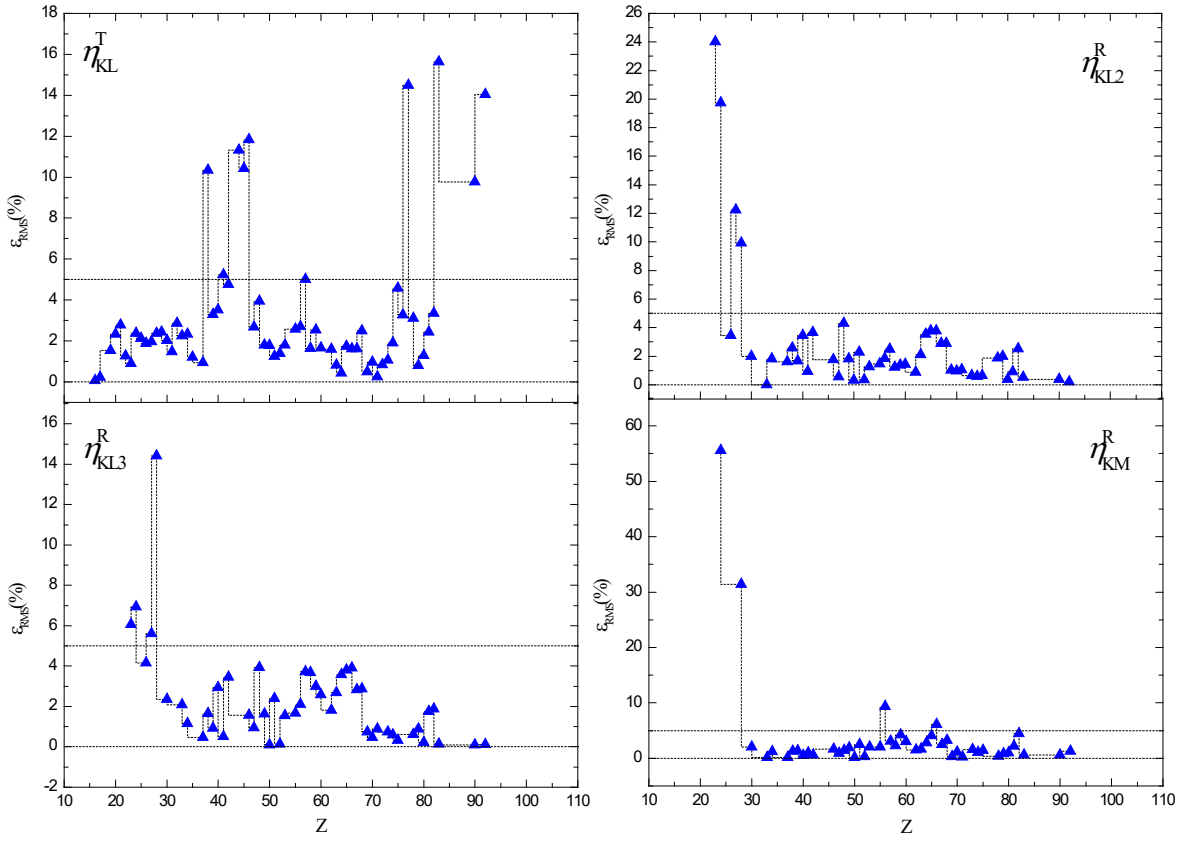

Fig. 6

Table 1. Summary of fitting coefficients and coefficients of determination (R^2) for calculating the semi-empirical values of vacancy transfer probabilities.

η	Z-group	The fitting coefficients according to eq (4)		The fitting coefficients according to eq (5)	
$\eta_{\mathrm{KL}}^{\mathrm{T}}$	16 to 92	A_0	2.43883	B_0	1.02081
		A_1	- 0,03711	B_1	- 0.00145
		A_2	3.40392×10^{-4}	B_2	1.64692×10^{-5}
		A_3	$1,41458\times10^{-5}$		
		A_4	$-9,10523\times10^{-8}$		
		R^2	0.99376		
$\eta_{\mathrm{KL2}}^{\mathrm{R}}$	23 to 92	A_0	- 0.40867	B_0	0.99074
		A_1	0.03019	B_1	6.75661×10^{-4}
		A_2	-4.96051×10^{-4}	B_2	-7.23948×10^{-6}
		A_3	3.49776×10^{-6}		
		A_4	-8.37308×10^{-9}		
		R^2	0.98460		
$\eta_{\mathrm{KL3}}^{\mathrm{R}}$	23 to 92	A_0	- 0.73512	B_0	0.98309
		A_1	0.05717	B_1	9.17699×10^{-4}
		A_2	-9.77319×10^{-4}	B_2	-8.52124×10^{-6}
		A_3	7.22962×10^{-6}		
		A_4	-1.98005×10^{-8}		
		R^2	0.99193		
$\eta_{\mathrm{KM}}^{\mathrm{R}}$	24 to 92	A_0	- 0.22884	B_0	0.94422
		A_1	0.01438	B_1	0.0023
		A_2	-2.12253×10^{-4}	B_2	-1.99925×10^{-5}
		A_3	1.53033×10^{-6}		
		A_4	-4.51053×10^{-9}		
		R^2	0.99221		

Table 2. Semi-empirical (this work), theoretical, fitted and experimental (other works) of total vacancy transfer probabilities η_{KL}^{T} from $_{16}$S to $_{92}$U.

Z, Symbol	This work		Other works					
	Semi-Empirical	$\varepsilon_{RMS}(\%)$	Theoretical (Berkani *et al*. 2025)	Empirical (Berkani *et al*. 2024)	Fitted (Schönfeld and JanBen 1996)	Experimental (Rao *et al*. 1972)		(Ertuğral *et al*. 2006)
Z=16, S	1.8132	0.07	1.82	1.7596	1.807			
Z=17, Cl	1.7731	0.22		1.7348	1.751			
Z=18, Ar	1.7336		1.74	1.7082	1.697			
Z=19, K	1.6947	1.53		1.6801	1.697			
Z=20, Ca	1.6564	2.33		1.6507	1.621	1.595		
Z=21, Sc	1.6188	2.77		1.6202	1.594			
Z=22, Ti	1.5820	1.26	1.61	1.5888	1.566	1.548		
Z=23, V	1.5459	0.89		1.5569	1.539			1.544
Z=24, Cr	1.5106	2.38		1.5244	1.508	1.495		1.509
Z=25, Mn	1.4762	2.13		1.4917	1.478		1.483[a]	1.467
Z=26, Fe	1.4425	1.88		1.4589	1.447	1.439	1.451[a]	1.453
Z=27, Co	1.4098	1.96		1.4262	1.418		1.418[a]	1.415
Z=28, Ni	1.3779	2.38		1.3938	1.388	1.375	1.388[a]	1.394
Z=29, Cu	1.3469	2.44	1.34	1.3617	1.357		1.357[a]	1.361
Z=30, Zn	1.3169	2.03	1.34	1.3301	1.326	1.316	1.327[a]	1.330
Z=31, Ga	1.2878	1.48		1.2992	1.294		1.298[a]	
Z=32, Ge	1.2597	2.87	1.28	1.2690	1.263	1.255	1.262[a]	
Z=33, As	1.2326	2.25	1.25	1.2397	1.232		1.231[a]	1.238
Z=34, Se	1.2064	2.32	1.22	1.2113	1.202	1.200	1.203[a]	1.204
Z=35, Br	1.1812	1.21		1.1840	1.174		1.174[a]	1.200
Z=36, Kr	1.1570		1.16	1.1579	1.149	1.149		
Z=37, Rb	1.1339	0.95		1.1329	1.125		1.128[a]	1.123
Z=38, Sr	1.1117	10.34		1.1091	1.102	1.104	1.102[a]	1.104
Z=39, Y	1.0905	3.29		1.0866	1.081		1.081[a]	
Z=40, Zr	1.0703	3.52	1.0727	1.0655	1.062	1.064	1.061[a]	1.064
Z=41, Nb	1.0511	5.24		1.0457	1.045		1.044[a]	1.042
Z=42, Mo	1.0329	4.76		1.0273	1.029	1.030	1.028[a]	1.026
Z=43, Tc	1.0157			1.0103	1.014			
Z=44, Ru	0.9995	11.31		0.9946	1.000	1.000		
Z=45, Rh	0.9842	10.42		0.9803	0.987			
Z=46, Pd	0.9699	11.84		0.9673	0.975	0.963		0.990
Z=47, Ag	0.9565	2.67		0.9556	0.964			0.967
Z=48, Cd	0.9440	3.95	0.957	0.9451	0.953	0.952		0.962
Z=49, In	0.9324	1.8		0.9359	0.944			0.950
Z=50, Sn	0.9217	1.77	0.936	0.9278	0.934	0.932		0.943
Z=51, Sb	0.9118	1.24		0.9208	0.925			0.924
Z=52, Te	0.9028	1.39	0.92	0.9147	0.917	0.914		0.923
Z=53, I	0.8945	1.8		0.9095	0.909			0.917
Z=54, Xe	0.8871			0.9051	0.902	0.899		
Z=55, Cs	0.8803	2.58		0.9014	0.895			
Z=56, Ba	0.8743	2.69		0.8982	0.888	0.887		0.882
Z=57, La	0.8689	5.01		0.8954	0.882			0.873
Z=58, Ce	0.8641	1.64		0.8929	0.876	0.876	0.874[b]	
Z=59, Pr	0.8600	2.54		0.8905	0.871		0.877[b]	
Z=60, Nd	0.8563	1.66		0.8880	0.866	0.865	0.872[b]	
Z=61, Pm	0.8532			0.8853	0.861			
Z=62, Sm	0.8505	1.59		0.8822	0.857	0.857	0.862[b]	
Z=63, Eu	0.8482	0.82		0.8785	0.853		0.853[b]	
Z=64, Gd	0.8463	0.44		0.8740	0.85	0.850	0.846[b]	
Z=65, Tb	0.8447	1.74		0.8685	0.847		0.851[b]	
Z=66, Dy	0.8433	1.62		0.8617	0.843	0.843	0.852[b]	
Z=67, Ho	0.8421	1.62		0.8535	0.841		0.841[b]	

Z=68, Er	0.8411	2.49		0.8435	0.838	0.836	0.843[b]
Z=69, Tm	0.8401	0.49		0.8315	0.835		0.836[b]
Z=70, Yb	0.8391	0.97		0.8173	0.833	0.831	0.831[b]
Z=71, Lu	0.8380	0.24		0.8388	0.831		0.836[b]
Z=72, Hf	0.8368	0.83		0.8359	0.829	0.826	0.827[b]
Z=73, Ta	0.8354	1.07		0.8327	0.827		0.822[b]
Z=74, W	0.8336	1.9		0.8294	0.825	0.821	0.823[b]
Z=75, Re	0.8316	4.57		0.8260	0.823		0.824[b]
Z=76, Os	0.8291	3.26		0.8224	0.821	0.816	
Z=77, Ir	0.8260	14.48		0.8186	0.819		0.819[b]
Z=78, Pt	0.8224	3.1		0.8146	0.818	0.813	
Z=79, Au	0.8180	0.79		0.8105	0.816		0.820[b]
Z=80, Hg	0.8129	1.29	0.811	0.8062	0.813	0.809	0.811[b]
Z=81, Tl	0.8069	2.43		0.8017	0.812		0.816[b]
Z=82, Pb	0.7999	3.36		0.7971	0.811	0.806	0.809[b]
Z=83, Bi	0.7918	15.63	0.805	0.7923	0.809		0.803[b]
Z=84, Po	0.7826			0.7873	0.807	0.805	
Z=85, At	0.7720			0.7822	0.805		
Z=86, Rn	0.7601		0.8	0.7769	0.804	0.802	
Z=87, Fr	0.7467			0.7714	0.803		
Z=88, Ra	0.7316			0.7658	0.801	0.798	
Z=89, Ac	0.7149			0.7600	0.799		
Z=90, Th	0.6962	9.77		0.7540	0.797	0.795	0.774[b]
Z=91, Pa	0.6756			0.7479	0.795		
Z=92, U	0.6529	14.04		0.7416	0.794	0.793	0.770[b]

[a](Öz 2006)
[b](Ertuğral *et al*. 2005)

Table 3. Semi-empirical (this work), theoretical, and experimental (other works) of radiative vacancy transfer probabilities η_{KL2}^{R} from $_{23}$V to $_{92}$U.

Z, Symbol	This work		Other works			
	Semi-Empirical	$\varepsilon_{RMS}(\%)$	Theoretical (Berkani *et al*. 2025)	Experimental (Rao *et al*. 1972)		Empirical (Berkani *et al*. 2024)
Z=23, V	0.0637	24.02				0.0715
Z=24, Cr	0.0760	19.74		0.083		0.0835
Z=25, Mn	0.0877					0.0950
Z=26, Fe	0.0989	3.44		0.103		0.1059
Z=27, Co	0.1096	12.23				0.1163
Z=28, Ni	0.1199	9.92		0.123		0.1261
Z=29, Cu	0.1296		0.1348			0.1355
Z=30, Zn	0.1389	1.98	0.144	0.142	0.138[a]	0.1444
Z=31, Ga	0.1477					0.1529
Z=32, Ge	0.1561		0.161	0.159		0.1608
Z=33, As	0.1640	0.00	0.169		0.164[a]	0.1684
Z=34, Se	0.1716	1.82	0.176	0.175		0.1756
Z=35, Br	0.1787					0.1823
Z=36, Kr	0.1855		0.19	0.188		0.1887
Z=37, Rb	0.1919	1.62			0.195[a]	0.1947
Z=38, Sr	0.1979	2.58		0.2	0.203[a]	0.2004
Z=39, Y	0.2036	1.67			0.207[a]	0.2057
Z=40, Zr	0.2090	3.45	0.2115	0.211	0.211[a]	0.2108
Z=41, Nb	0.2140	0.93			0.216[b]	0.2155
Z=42, Mo	0.2187	3.66		0.220	0.218[b]	0.2199
Z=43, Tc	0.2232					0.2241
Z=44, Ru	0.2274			0.227		0.2280
Z=45, Rh	0.2313					0.2316
Z=46, Pd	0.2349	1.75		0.234	0.239[b]	0.2350
Z=47, Ag	0.2383	0.55			0.237[b]	0.2382
Z=48, Cd	0.2415	4.31	0.241	0.240	0.239[b]	0.2411
Z=49, In	0.2444	1.80			0.240[b]	0.2439
Z=50, Sn	0.2472	0.32	0.245	0.245	0.248[b]	0.2465
Z=51, Sb	0.2497	2.28			0.244[b]	0.2489
Z=52, Te	0.2521	0.36	0.25	0.249	0.253[b]	0.2511
Z=53, I	0.2542	1.26			0.251[b]	0.2532
Z=54, Xe	0.2562			0.253		0.2551
Z=55, Cs	0.2581	1.45			0.254[b]	0.2569
Z=56, Ba	0.2598	1.85		0.256	0.255[b]	0.2586
Z=57, La	0.2614	2.49			0.257[b]	0.2602
Z=58, Ce	0.2628	1.23		0.259	0.259[b]	0.2616
Z=59, Pr	0.2641	1.37			0.261[b]	0.2630
Z=60, Nd	0.2653	1.44		0.261	0.264[c]	0.2642
Z=61, Pm	0.2664					0.2654
Z=62, Sm	0.2675	0.88		0.264	0.265[c]	0.2665
Z=63, Eu	0.2684	2.11			0.266[c]	0.2676
Z=64, Gd	0.2693	3.55		0.266	0.267[c]	0.2686
Z=65, Tb	0.2701	3.78				0.2695
Z=66, Dy	0.2708	3.77		0.268	0.269[c]	0.2704
Z=67, Ho	0.2715	2.89			0.269[c]	0.2712
Z=68, Er	0.2722	2.89		0.27	0.270[c]	0.2721
Z=69, Tm	0.2728	1.03			0.270[d]	0.2729
Z=70, Yb	0.2734	0.95		0.272	0.272[c]	0.2737
Z=71, Lu	0.2739	1.06			0.271[d]	0.2744
Z=72, Hf	0.2745			0.274		0.2752
Z=73, Ta	0.2751	0.64			0.274[c]	0.2759
Z=74, W	0.2756	0.58		0.275	0.274[c]	0.2767

Z=75, Re	0.2762	0.65			0.278[d]	0.2775
Z=76, Os	0.2767			0.277		0.2782
Z=77, Ir	0.2773					0.2790
Z=78, Pt	0.2779	1.86		0.278		0.2798
Z=79, Au	0.2786	1.98			0.278[d]	0.2806
Z=80, Hg	0.2793	0.37	0.28	0.28	0.280[c]	0.2815
Z=81, Tl	0.2800	0.90				0.2823
Z=82, Pb	0.2807	2.50		0.281	0.281[c]	0.2832
Z=83, Bi	0.2815	0.53	0.281		0.280[d]	0.2841
Z=84, Po	0.2824			0.284		0.2851
Z=85, At	0.2833					0.2860
Z=86, Rn	0.2843		0.284	0.285		0.2870
Z=87, Fr	0.2853					0.2881
Z=88, Ra	0.2864			0.286		0.2891
Z=89, Ac	0.2876					0.2902
Z=90, Th	0.2889	0.38		0.288	0.290[d]	0.2914
Z=91, Pa	0.2902					0.2925
Z=92, U	0.2916	0.21		0.289	0.291[d]	0.2937

[a](Ertuğrul 2002d)

[b](Çalilskan *et al*. 2002)

[c](Durak and Özdemir 1998)

[d](Ertuğrul *et al*. 1997a)

Table 4. Semi-empirical (this work), theoretical, and experimental (other works) of radiative vacancy transfer probabilities η^{R}_{KL3} from $_{23}$V to $_{92}$U.

Z, Symbol	This work		Other works			
	Semi-Empirical	$\varepsilon_{RMS}(\%)$	Theoretical (Berkani *et al*. 2025)	Experimental (Rao *et al*. 1972)		Empirical (Berkani *et al*. 2024)
Z=23, V	0.1452	6.06				0.1447
Z=24, Cr	0.1674	6.93		0.165		0.1669
Z=25, Mn	0.1887					0.1881
Z=26, Fe	0.2089	4.16		0.203		0.2083
Z=27, Co	0.2282	5.61				0.2275
Z=28, Ni	0.2465	14.40		0.242		0.2458
Z=29, Cu	0.2639		0.2637			0.2631
Z=30, Zn	0.2804	2.35	0.2815	0.279	0.270[a]	0.2795
Z=31, Ga	0.2960					0.2951
Z=32, Ge	0.3108		0.3133	0.311		0.3099
Z=33, As	0.3248	2.09	0.3283		0.318[a]	0.3239
Z=34, Se	0.3381	1.14	0.342	0.340	0.333[a]	0.3370
Z=35, Br	0.3505					0.3495
Z=36, Kr	0.3623		0.3661	0.365		0.3612
Z=37, Rb	0.3733	0.46			0.375[a]	0.3722
Z=38, Sr	0.3837	1.64		0.387	0.390[a]	0.3826
Z=39, Y	0.3934	0.92			0.397[a]	0.3923
Z=40, Zr	0.4024	2.93	0.405	0.405	0.404[a]	0.4014
Z=41, Nb	0.4109	0.51			0.413[b]	0.4098
Z=42, Mo	0.4188	3.45		0.421	0.416[b]	0.4177
Z=43, Tc	0.4261					0.4251
Z=44, Ru	0.4329			0.433		0.4319
Z=45, Rh	0.4392					0.4383
Z=46, Pd	0.4450	1.57		0.443	0.452[b]	0.4441
Z=47, Ag	0.4503	0.95			0.446[b]	0.4495
Z=48, Cd	0.4551	3.92	0.4536	0.452	0.451[b]	0.4544
Z=49, In	0.4595	1.63			0.452[b]	0.4589
Z=50, Sn	0.4636	0.09	0.46	0.460	0.464[b]	0.4630
Z=51, Sb	0.4672	2.40			0.456[b]	0.4667
Z=52, Te	0.4704	0.13	0.4659	0. 465	0.471[b]	0.4701
Z=53, I	0.4733	1.54			0.466[b]	0.4731
Z=54, Xe	0.4759			0.469		0.4758
Z=55, Cs	0.4782	1.67			0.469[b]	0.4781
Z=56, Ba	0.4801	2.10		0.473	0.470[b]	0.4802
Z=57, La	0.4818	3.71			0.470[b]	0.4820
Z=58, Ce	0.4832	3.67		0.475	0.475[b]	0.4835
Z=59, Pr	0.4844	3.00			0.477[b]	0.4848
Z=60, Nd	0.4853	2.58		0.477	0.480[c]	0.4859
Z=61, Pm	0.4860					0.4867
Z=62, Sm	0.4865	1.81		0.479	0.481[c]	0.4873
Z=63, Eu	0.4869	2.68			0.481[c]	0.4877
Z=64, Gd	0.4870	3.58		0.479	0.482[c]	0.4880
Z=65, Tb	0.4870	3.81				0.4881
Z=66, Dy	0.4868	3.90		0.480	0.483[c]	0.4880
Z=67, Ho	0.4865	2.83			0.482[c]	0.4878
Z=68, Er	0.4861	2.87		0.479	0.482[c]	0.4875
Z=69, Tm	0.4856	0.74			0.482[d]	0.4870
Z=70, Yb	0.4850	0.46		0.480	0.482[c]	0.4865
Z=71, Lu	0.4842	0.87			0.480[d]	0.4858
Z=72, Hf	0.4834			0.479		0.4851
Z=73, Ta	0.4825	0.73			0.480[c]	0.4842
Z=74, W	0.4816	0.58		0.478	0.480[c]	0.4833

Z=75, Re	0.4806	0.33			0.479[d]	0.4824
Z=76, Os	0.4796			0.478		0.4813
Z=77, Ir	0.4785					0.4803
Z=78, Pt	0.4774	0.61		0.477		0.4791
Z=79, Au	0.4763	0.89			0.478[d]	0.4780
Z=80, Hg	0.4751	0.21	0.4755	0.476	0.476[c]	0.4768
Z=81, Tl	0.4739	1.74				0.4755
Z=82, Pb	0.4728	1.88		0.475	0.474[c]	0.4743
Z=83, Bi	0.4716	0.13	0.4732		0.471[d]	0.4730
Z=84, Po	0.4704			0.474		0.4717
Z=85, At	0.4693					0.4704
Z=86, Rn	0.4681		0.4695	0. 473		0.4691
Z=87, Fr	0.4670					0.4678
Z=88, Ra	0.4658			0.472		0.4665
Z=89, Ac	0.4647					0.4652
Z=90, Th	0.4636	0.09		0.470	0.464[d]	0.4638
Z=91, Pa	0.4625					0.4625
Z=92, U	0.4615	0.11		0.469	0.462[d]	0.4611

[a](Ertuğrul 2002d)

[b](Çalilskan *et al*. 2002)

[c](Durak and Özdemir 1998)

[d](Ertuğrul *et al*. 1997a)

Table 5. Semi-empirical (this work), theoretical, and experimental (other works) of radiative vacancy transfer probabilities η_{KM}^{R} from $_{24}$Cr to $_{92}$U.

Z, Symbol	This work		Other works		
	Semi-Empirical	$\varepsilon_{rms}(\%)$	Experimental (Rao *et al*., 1972)		Empirical (Berkani *et al*. 2024)
Z=24, Cr	0.0135	55.56			0.0139
Z=25, Mn	0.0199				0.0202
Z=26, Fe	0.0261		0.0371		0.0263
Z=27, Co	0.0321				0.0322
Z=28, Ni	0.0379	31.40			0.0380
Z=29, Cu	0.0436				0.0435
Z=30, Zn	0.0490	2.04	0.0532	0.050[a]	0.0488
Z=31, Ga	0.0542				0.0540
Z=32, Ge	0.0592		0.0624		0.0590
Z=33, As	0.0641	0.16		0.064[a]	0.0638
Z=34, Se	0.0688	1.16		0.068[a]	0.0685
Z=35, Br	0.0733				0.0730
Z=36, Kr	0.0777		0.0806		0.0773
Z=37, Rb	0.0819	0.12		0.082[a]	0.0815
Z=38, Sr	0.0859	1.28		0.087[a]	0.0855
Z=39, Y	0.0898	1.34		0.091[a]	0.0894
Z=40, Zr	0.0935	0.53	0.0967	0.094[a]	0.0931
Z=41, Nb	0.0971	0.93		0.098[b]	0.0967
Z=42, Mo	0.1006	0.60	0.104	0.10[b]	0.1002
Z=43, Tc	0.1039				0.1035
Z=44, Ru	0.1071				0.1067
Z=45, Rh	0.1102				0.1098
Z=46, Pd	0.1131	1.68		0.115[b]	0.1127
Z=47, Ag	0.1160	0.86	0.119	0.115[b]	0.1156
Z=48, Cd	0.1187	1.43		0.117[b]	0.1183
Z=49, In	0.1213	1.90		0.119[b]	0.1209
Z=50, Sn	0.1238	0.16	0.126	0.124[b]	0.1234
Z=51, Sb	0.1261	2.46		0.123[b]	0.1258
Z=52, Te	0.1284	0.31		0.128[b]	0.1281
Z=53, I	0.1306	1.99		0.128[b]	0.1303
Z=54, Xe	0.1327				0.1324
Z=55, Cs	0.1347	2.06		0.131[b]	0.1344
Z=56, Ba	0.1366	9.33	0.137	0.133[b]	0.1363
Z=57, La	0.1384	3.11		0.134[b]	0.1382
Z=58, Ce	0.1402	2.25		0.137[b]	0.1399
Z=59, Pr	0.1418	4.18		0.138[b]	0.1416
Z=60, Nd	0.1434	2.99	0.143	0.142[c]	0.1432
Z=61, Pm	0.1449				0.1447
Z=62, Sm	0.1463	1.46		0.144[c]	0.1462
Z=63, Eu	0.1477	1.63		0.144[c]	0.1476
Z=64, Gd	0.1490	2.76		0.146[c]	0.1489
Z=65, Tb	0.1502	4.04	0.149		0.1501
Z=66, Dy	0.1514	6.11		0.148[c]	0.1513
Z=67, Ho	0.1525	2.48		0.150[c]	0.1524
Z=68, Er	0.1535	3.21		0.151[c]	0.1535
Z=69, Tm	0.1545	0.32		0.154[d]	0.1545
Z=70, Yb	0.1554	1.13	0.154	0.153[c]	0.1555
Z=71, Lu	0.1563	0.19		0.156[d]	0.1564
Z=72, Hf	0.1571				0.1573
Z=73, Ta	0.1579	1.55		0.156[c]	0.1581
Z=74, W	0.1586	1.01		0.157[c]	0.1588
Z=75, Re	0.1593	1.44		0.157[d]	0.1596

Z=76, Os	0.1599			0.1603
Z=77, Ir	0.1605			0.1609
Z=78, Pt	0.1610	0.36		0.1615
Z=79, Au	0.1615	0.82	0.160[d]	0.1621
Z=80, Hg	0.1620	0.98	0.161[c]	0.1626
Z=81, Tl	0.1624	2.14		0.1631
Z=82, Pb	0.1627	4.45	0.163[c]	0.1636
Z=83, Bi	0.1630	0.61	0.162[d]	0.1641
Z=84, Po	0.1633			0.1645
Z=85, At	0.1635			0.1649
Z=86, Rn	0.1637			0.1652
Z=87, Fr	0.1638			0.1656
Z=88, Ra	0.1639			0.1659
Z=89, Ac	0.1640			0.1662
Z=90, Th	0.1640	0.61	0.163[d]	0.1664
Z=91, Pa	0.1640			0.1667
Z=92, U	0.1639	1.28	0.166[d]	0.1669

[a](Ertuğrul 2002d)

[b](Çalilskan *et al*. 2002)

[c](Durak and Özdemir 1998)

[d](Ertuğrul *et al*. 1997a)